Journal of Magnetic Resonance **155,** 251–256 (2002)
doi:10.1006/jmre.2002.2524, available online at http://www.idealibrary.com on IDEAL®

Simultaneous Selective Detection of Multiple Quantum Spectra

R. T. Syvitski,* N. Burlinson,* E. E. Burnell,* and J. Jeener†

*Department of Chemistry, University of British Columbia, 2036 Main Mall, Vancouver, British Columbia, Canada, V6T 1Z1; and †Université Libre de Bruxelles (CP-232), B-1050 Brussels, Belgium

E-mail: elliott.burnell@ubc.ca

Received August 13, 2001; revised March 6, 2002

A three-dimensional multiple-quantum NMR experiment that produces individual spectra of all quantum orders is described. The separation of different quantum orders is accomplished via Fourier transformation with respect to the phase of the first two pulses of a generic three-pulse multiple-quantum sequence. This dramatically reduces the time required to obtain several selectively detected spectra and enhances the sensitivity and digital resolution from that obtained using the original two-dimensional technique. The experiment is demonstrated on the protons of *para*-chlorotoluene dissolved in the nematic liquid crystal Merck ZLI-1132.

Key Words: **liquid crystal; nematic; NMR; MQNMR; orientational order; multiple quantum coherence.**

1. INTRODUCTION

The NMR spectra of solute molecules that are orientationally ordered in liquid crystalline solvents provide a wealth of information that is unavailable from high-resolution NMR spectra of isotropic liquids, and that is obscured by the broad, featureless NMR spectra obtained from solid materials. In particular, accurate molecular structures and information on orientational ordering are available from the dipolar and quadrupolar couplings that dominate the spectra of orientationally ordered fluids. In addition, anisotropies of spin–spin coupling and chemical shift tensors can be measured, as well as the absolute signs of indirect spin–spin coupling constants. The method also provides an indirect way of probing the relative conformer probabilities of flexible molecules in the liquid phase (*1–7*).

Unfortunately, the complexity of the NMR spectrum of an orientationally ordered solute increases dramatically with the number of spins. For example, a molecule such as butane that contains 10 spin 1/2 protons gives rise to a high-resolution NMR spectrum that contains thousands of lines (*7*). Thus high-resolution NMR spectroscopy of orientationally ordered solutes has been limited in general to the investigation of relatively small solutes dissolved in nematic liquid crystal solvents.

The technique of multiple quantum NMR (MQ-NMR) was proposed as an attractive means of dealing with more complicated spin systems. In the original versions of the technique, all quantum orders were collected simultaneously in a single, very broad spectrum that had very poor digital resolution (*8*). Later modifications to the phase cycling enabled the measurement of one selected quantum order with much higher digital resolution (*9, 10*); however, the time needed to acquire such a spectrum is roughly equal to that required for the original, nonselective experiment.

It has been suggested that all quantum orders can be measured simultaneously (as separate slices of a multidimensional spectrum) in an experiment that performs a Fourier analysis with respect to the phase incrementation of the preparation pulses (*8, 9, 11*). In this paper we demonstrate this suggestion using a 3D method that, similar to the original MQ-NMR method, simultaneously measures all MQ-NMR orders but with the excellent digital resolution of the selective experiment. We choose the seven-proton system of *para*-chlorotoluene to demonstrate the ideas.

2. EXPERIMENTAL

The solute *para*-chlorotoluene was dissolved in the nematic liquid crystal Merck ZLI-1132 (*4*) which was then placed inside a 5-mm outer diameter NMR tube with a capillary containing d_6-acetone (to provide a field-frequency lock signal) in the center. Spectra were run on a Bruker AMX-500 high-resolution pulsed NMR spectrometer, and temperature was controlled and maintained at 300 K using the standard air-flow system. For all experiments the recycle delay was 1.5 s, the 90° pulse width varied between 10 and 10.5 μs, and 1024 complex points were acquired for each variable increment. The proton spin–lattice relaxation times of the various transitions in *para*-chlorotoluene varied from about 1.4 s for the methyl protons to about 2.4 s for the aromatic protons.

3. RESULTS AND DISCUSSION

The simplest way to obtain a multiple-quantum NMR spectrum is to use the pulse sequence of Fig. 1 with phases ϕ

1090-7807/02 $35.00

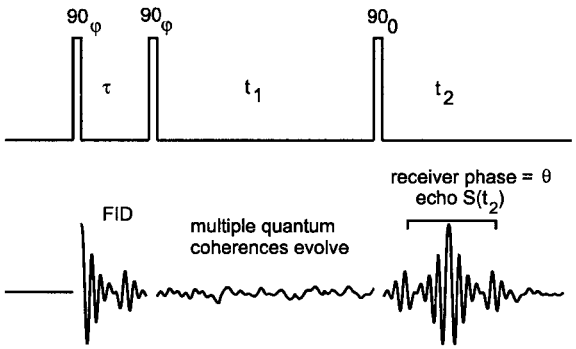

FIG. 1. The pulse sequences used in this paper are all variants of the sequence shown, with phase cycling as described in Table 1. Sequence A is a simple example of a generic three-pulse sequence, any of which can in general produce a MQ-NMR spectrum. In general, some of the MQ-NMR coherences that are generated by the second pulse, and that evolve during the variable time t_1, are transferred back into observable coherences by the third pulse. The MQ-NMR spectrum is obtained by Fourier transforming as a function of t_1 the echo signal that follows the third pulse. In practice this is accomplished via a 2D transform of the signals acquired as a function of t_1 and t_2. The absolute value of the summed projection onto the F_1 axis is then the MQ-NMR spectrum, as shown in Fig. 2.

and θ kept constant, and to perform a two-dimensional (2D) Fourier transform of the signals $S(t_2)$ collected as a function of varying t_1 (sequence A of Table 1). The absolute value of the summed projection onto the F_1 axis is then the spectrum of coherences that are evolving between the second and third pulses. Figure 2 presents the MQ-NMR spectrum of *para*-chlorotoluene obtained from such a 2D experiment. Both positive and negative multiple-quantum orders are obtained. The problem with MQ-NMR spectra obtained in this manner is that the wide spectral width (1 MHz is required in this case by the large orientational order of *para*-chlorotoluene) and large spectral offset (required to separate the various orders) give rise to very poor digital resolution (61 Hz per point in Fig. 2). These conditions also produce poor signal to noise in the resulting MQ-NMR spectrum.

TABLE 1
Phase Cycles for the Three Pulse Sequences[a]

Sequence	Phase	Phase list
A[b]	ϕ	0
	θ	0
B[c]	ϕ	$0,\ 90/N,\ 2\times 90/N,\ 3\times 90/N \ldots (4N-1)\times 90/N$
	θ	0, 90, 180, 270
C[d]	ϕ	$0,\ 360/n,\ 2\times 360/n,\ 3\times 360/n \ldots (n-1)\times 360/n$
	θ	0

[a] As defined in Fig. 1, ϕ refers to the phase of pulses 1 and 2, and θ refers to the receiver phase.

[b] Sequence A gives all MQ orders in a single, wide spectrum (see, e.g., Fig. 2). For this experiment the phases ϕ and θ can be any arbitrary constant angle. Zero degrees was chosen for convenience.

[c] Sequence B is used for the selective detection of the NQ (and $2NQ$, $3NQ \ldots$) spectrum. N is the quantum order being selectively detected.

[d] Sequence C is used for the 3D experiment, where n is an arbitrary integer that should be at least $2N_{\max}+1$. A separate signal is acquired and stored for each value of n, giving a three-dimensional interferogram that is a function of t_1, ϕ, and t_2.

The problems of large offset and spectral width can be alleviated somewhat by selectively detecting a specific NQ spectrum (where N is the MQ order); this spectrum can be measured via a pulse sequence in which the phase of the first two pulses is incremented by $360/N$ degrees with N scans per t_1 increment, and with the signals following the third pulse co-added. In this case the $0, \pm N, \pm 2N \ldots$ quanta spectra will be obtained, with the signals from all other orders adding to zero. The $0Q$ spectrum can be canceled by doubling the number of scans per t_1 increment (to $2N$), halving the size (to $180/N$ degrees) of the phase increment of the first two pulses, and alternately adding and subtracting the echo signal. Furthermore, the negative orders can be eliminated by the pulse sequence (sequence B of Table 1) in which for each value of t_1 the phase of the first two pulses ϕ is incremented by $90/N$ degrees with $4N$ scans per t_1 increment while the receiver phase is cycled 0, 90, 180, 270 degrees. The signals from all except orders $+N,\ +2N \ldots$ add to zero. The cancellation occurs because the phase of the detected quantum order N following pulse 2 is shifted by $N\times\phi$. Hence, as ϕ is incremented by $90/N$ degrees, the phase of the quantum order N is incremented by 90°. As the receiver phase is also incremented by 90°, the signals from order $+N$ (and $+2N,\ +3N \ldots$) add constructively, while the signals from all other quantum orders are canceled. Hence, only multiples of the quantum order $+N$ contribute to the signal obtained over a full phase cycle (*10*).

Figure 3 gives the selective detection $+4Q$ and $+6Q$ spectra of *para*-chlorotoluene obtained using the selective detection pulse sequence B. Figure 3 includes for comparison expansions from Fig. 2 of these same orders obtained using the nonselective pulse sequence A. The improvement in spectral quality achieved with selective detection is quite dramatic; the digital resolution and the signal to noise are both improved. However, because the total experiment must be repeated for each selectively detected MQ-NMR spectrum desired, the total time taken to observe all important orders (the highest three orders are most important for determining spectral parameters) is greatly increased. For example, the time taken for the selective $+4Q$ spectrum of Fig. 3 is equal to that required to obtain the nonselective spectrum of all orders in Fig. 2. In each selective detection experiment, information about any except the desired MQ-NMR order has been removed (i.e., thrown away) by the add/subtract effect of the receiver phase cycling.

It is possible to perform the selective detection experiment in such a manner as to obtain spectra of all orders simultaneously. Instead of adding/subtracting echo signals as in sequence B, individual echoes $S(t_2)$ are acquired as a function of t_1 and of ϕ, where ϕ is incremented by $360/n$ degrees n times for each t_1 value (sequence C) (*8*). This gives rise to a 3-dimensional interferogram, where the acquired signal is a function of t_1,

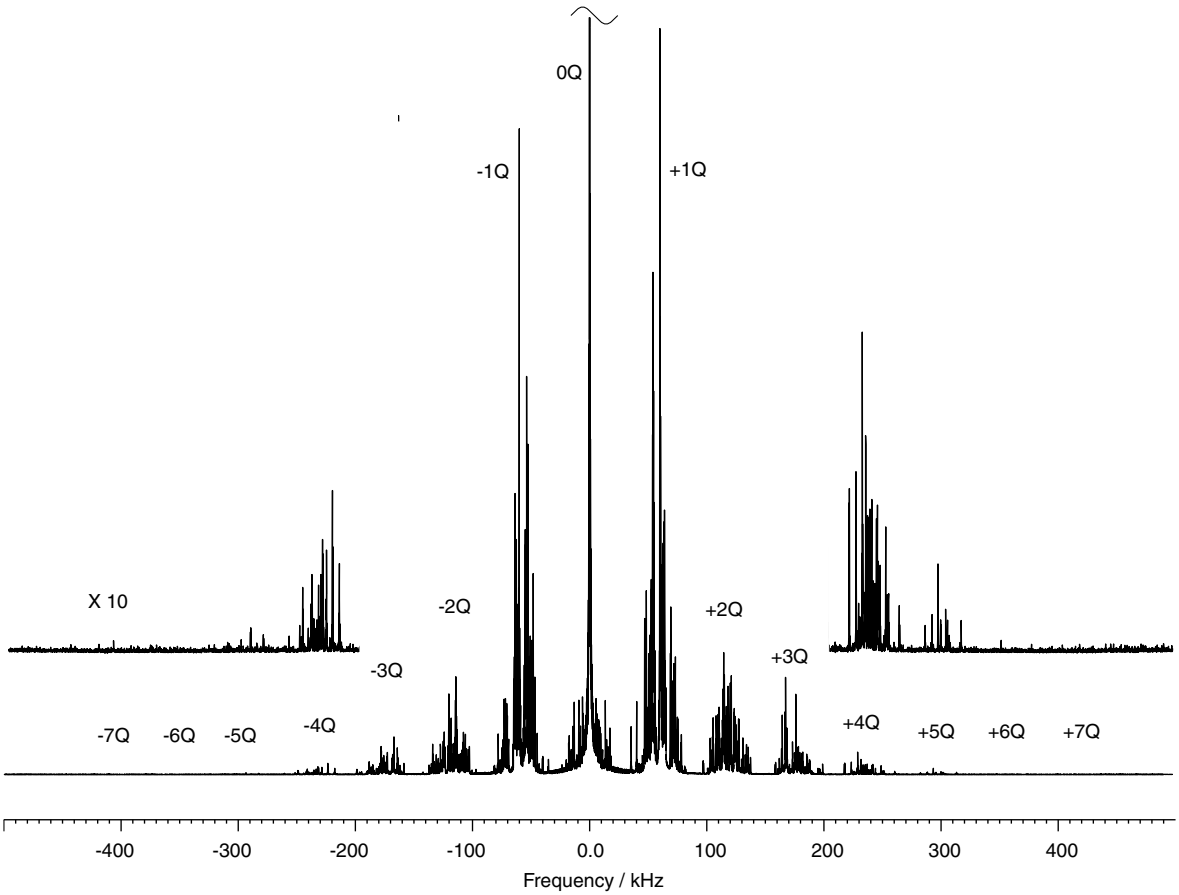

FIG. 2. Multiple-quantum spectrum of *para*-chlorotoluene in ZLI-1132. This spectrum was collected in 14 h 5 m using sequence A (Fig. 1, Table 1) with τ set to 20 ms, four scans/t_1 increment, 8192 t_1 increments, F_2 spectral width of 83333 Hz, and F_1 spectral width of 1 MHz. The absolute value of the projection of the complex F_2 spectra onto the F_1 axis gives the F_1 spectrum, which is the entire MQ-NMR spectrum. The spectrometer frequency was offset by 60000 Hz from the center of the spectrum in order to separate the various orders. Under these conditions, the higher order coherences are poorly detected, presumably due to the combination of the large offset with the long duration (10 μs) of the 90° pulses.

ϕ, and the acquisition time t_2. After Fourier transforming with respect to t_1, ϕ, and t_2, the Fourier transforms of the echo signals F_3 are summed onto the F_1 dimension; the absolute values of the ϕ slices of this projection are the desired MQ-NMR spectra which occur at "pseudo frequencies" N, as demonstrated for *para*-chlorotoluene for slices 9 to 16 in Fig. 4 (spectra for the $-7Q$ to $-1Q$ orders are not shown). This experiment, which measures all quantum orders at the same time, took precisely the same time as the nonselective experiment of Fig. 2 and as the selective $+4Q$ spectrum of Fig. 3.

The quality of the spectra obtained can be judged in Fig. 3, where the $+4Q$ and $+6Q$ spectra obtained using the pulse sequences A and B are compared with those obtained from a three-dimensional experiment using pulse sequence C. There is no loss in digital resolution or spectral quality when using the three-dimensional approach C rather than the usual coaddition approach B, but the approach C has the tremendous advantage of a large reduction in total acquisition time (which no longer increases proportional to the number of different MQ-NMR spectra required), and the additional benefit of simultaneous acquisition of all selective spectra at precisely the same sample and spectrometer conditions.

Two factors contribute to the much poorer quality of the "sequence A" spectrum shown in Figs. 2 and 3A. First, the spectral resolution is severely limited by the very large width (about 1 MHz) of this indirectly detected spectrum. The other difficulty arises from the combination of the 10 μs 90° pulse width (that is inherent in the use of a standard high-resolution NMR spectrometer) with the large "chemical shift" offset (60 kHz) that is required to separate the spectra from different MQ orders. To illustrate the problem, consider the motion of a free proton with the average chemical shift of protons in *para*-chlorotoluene, during such an offset irradiation. In the appropriate frame rotating at the irradiation frequency, this motion combines a rotation around X at 25 kHz (1/4 turn in 10 μs) with a rotation around Z at 60 kHz (the offset), which results in an overall Rabi rotation at 65 kHz (hence, $\approx$234° in 10 μs) around an axis in the XZ plane, tilted by $\approx$22.6° from Z. This somewhat complicated motion,

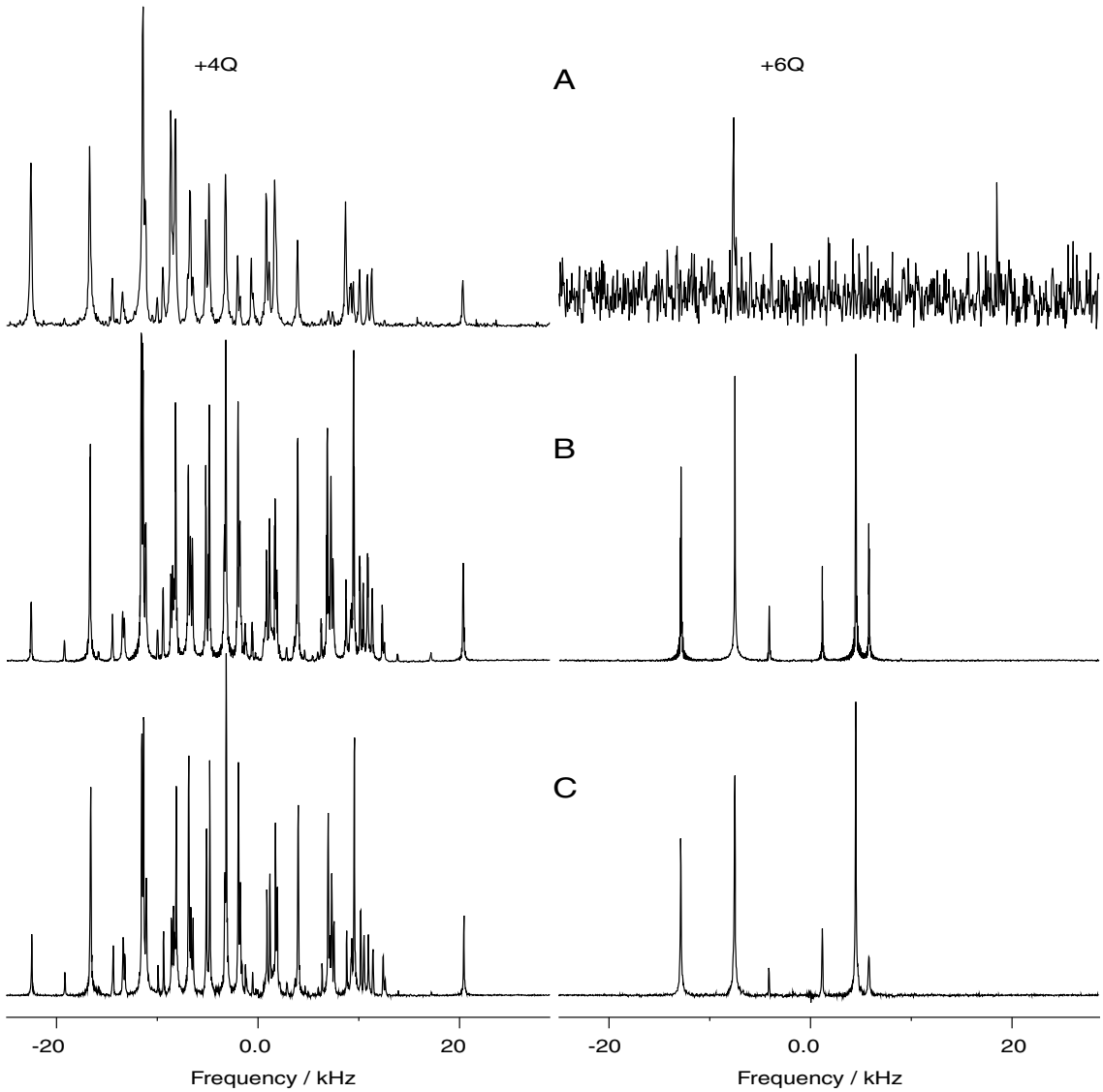

FIG. 3. Comparison of the $+4Q$ and $+6Q$ MQ-NMR spectra obtained with different techniques. A is from Fig. 2 and was obtained using sequence A. The line at ≈18 kHz in the $6Q$ spectrum is an artifact (equivalent to the noise observed in Fig. 2). B is the absolute value of the spectrum obtained from a selective detection of the $+4Q$ complex spectrum requiring 14 h 10 m (and the $+6Q$ complex spectrum requiring another 10 h 40 m) obtained using sequence B with N equal 4 (and 6), τ set to 20 ms, two (and one) scans for each of 16 (and 24) phase increments per t_1 increment, 1024 t_1 increments, F_1 spectral width of 33333 Hz, and F_1 spectral width of 70 kHz. C gives two slices of the absolute value of the 3D experiment (displayed in Fig. 4) obtained using sequence C. The intensity differences between the $6Q$ spectra obtained using sequences B and C are most likely due to spectrometer fluctuations. For comparison, the ratios of vertical scales for the $6Q$ to the $4Q$ spectra are 17 × for A, 1.35 × for B, and 1.42 × for C. One zero filling was applied to the t_1 signals before the Fourier transform. The digital resolution is then 61 Hz per point in A and 34 Hz per point in B and C. The peaks of very strong lines have been chopped off for clarity.

acting on a vector which points initially in the Z direction, leaves this vector tilted by ≈40.1° from the Z axis at the end of the 10 μs pulse (instead of the "nominal" value of 90°). For ideal hard pulses of small tipping angle θ, the efficiency of the generation or observation of n-quantum coherences is known to be proportional to $\theta^{|n|}$. This provides a simple qualitative interpretation for the strong decrease in signal intensity seen in Fig. 2 for the higher values of $|n|$. A quantitative interpretation for the intensities of all lines, for all the experiments presented here, would require a numerical calculation (which we have not performed) involving pulse duration, offset, and the complete spin Hamiltonian.

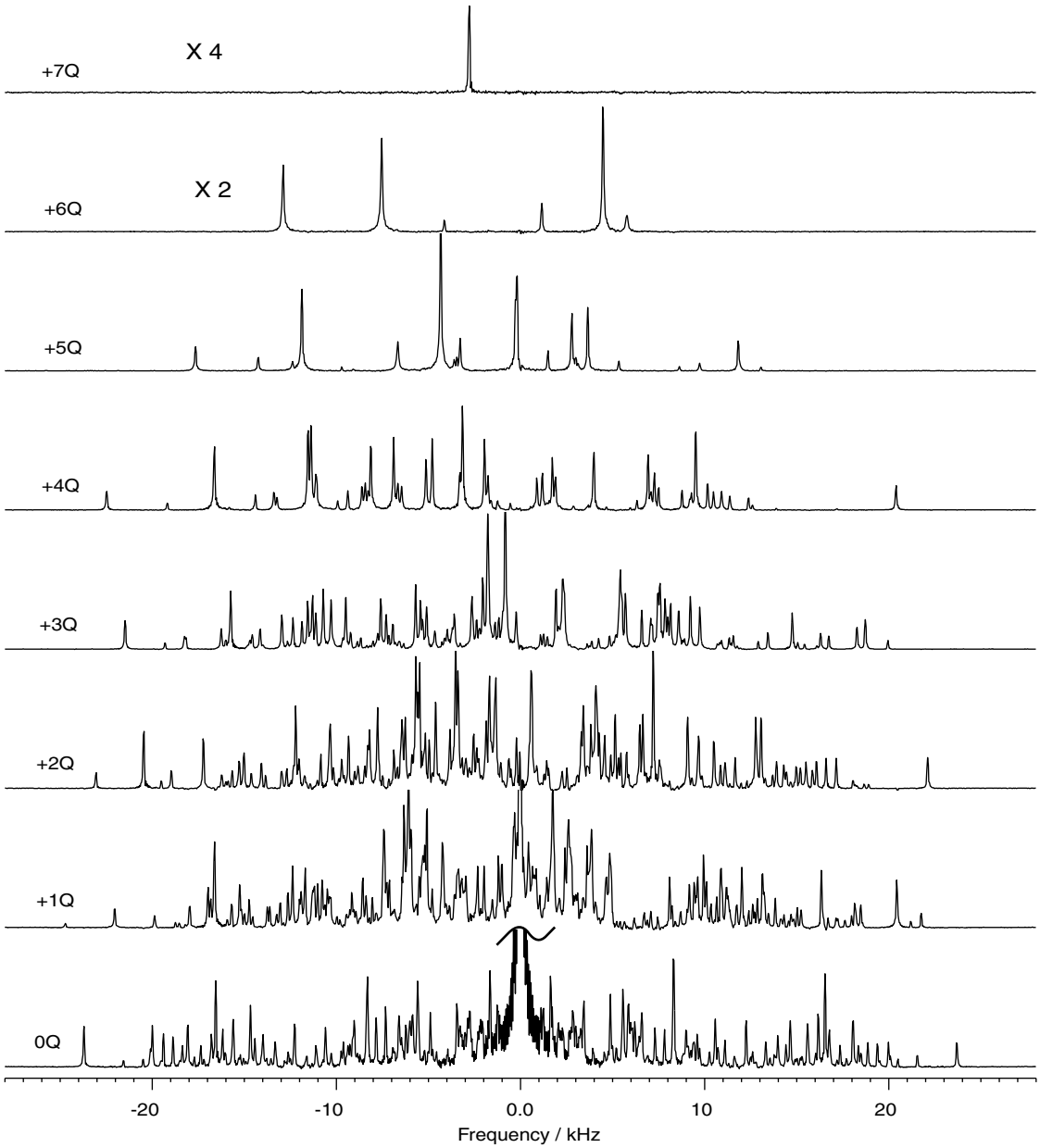

FIG. 4. Absolute values of multiple-quantum spectra obtained in 14 h 25 m from the 3D experiment using sequence C with τ set to 20 ms, two scans for each of $n = 16$ phase increments per t_1 increment, 1024 t_1 increments, F_3 spectral width of 33333 Hz, and F_1 spectral width of 70 kHz. The Fourier transforms F_3 of the echo signals $S(t_2)$ have been summed onto the F_1 dimension. The absolute value of the result is a 2-dimensional spectrum where F_2 are the pseudo ϕ spectra, and F_1 the desired multiple quantum spectra. The positive MQ-NMR orders (F_1 slices 9 to 16) are shown, which correspond to the 0 to $+7Q$ spectra. The peaks of very strong lines have been chopped off for clarity.

ACKNOWLEDGMENTS

RTS and EEB are grateful to The Natural Sciences and Engineering Research Council of Canada (NSERC) for financial support. We are also grateful to the E. Merck Company of Darmstadt, Germany, for their gift of the nematic liquid crystal, Merck ZLI–1132.

REFERENCES

1. A. D. Buckingham and K. A. McLauchlan, High resolution nuclear magnetic resonance in partially oriented molecules, *Prog. Nuclear Magn. Reson. Spectrosc*. **2,** 63–109 (1967).

2. P. Diehl and C. L. Khetrapal, NMR studies of molecules oriented in the nematic phase of liquid crystals, *in* "NMR Basic Principles and Progress" (P. Diehl, E. Fluck, and R. Kosfeld, Eds.), Vol. 1, pp. 1–95, Springer-Verlag, Berlin (1969).

3. J. W. Emsley and J. C. Lindon, "NMR Spectroscopy Using Liquid Crystal Solvents," Pergamon Press, Oxford (1975).

4. J. Lounila and J. Jokisaari, Anisotropies in spin–spin coupling constants and chemical shifts as determined from the nmr spectra of molecules oriented by

liquid crystal solvents, *Prog. Nuclear Magn. Reson. Spectrosc.* **15,** 249–290 (1982).

5. R. Y. Dong, "Nuclear Magnetic Resonance of Liquid Crystals," 2nd ed., Springer-Verlag, New York (1997).
6. E. E. Burnell and C. A. de Lange, Prediction from molecular shape of solute orientational order in liquid crystals, *Chem. Rev.* **98,** 2359–2387 (1998).
7. J. M. Polson and E. E. Burnell, Conformational equilibrium and orientational ordering: ^{1}H-nuclear magnetic resonance of butane in a nematic liquid crystal, *J. Chem. Phys.* **103,** 6891–6902 (1995).
8. D. P. Weitekamp, Time-domain multiple-quantum NMR, *Adv. Magn. Reson.* **11,** 111 (1983).
9. A. Wokaun and R. R. Ernst, Selective detection of multiple quantum transitions in NMR by two-dimensional spectroscopy, *Chem. Phys. Lett.* **52,** 407–412 (1977).
10. L. W. Field and M. L. Terry, Multiple-quantum NMR spectroscopy of molecules aligned in liquid crystal solvents. Selective quadrature detection of multiple-quantum spectra, *J. Magn. Reson.* **69,** 176–179 (1986).
11. D. N. Shykind, J. Baum, S.-B. Liu, and A. Pines, Phase-incremented multiple-quantum nmr experiments, *J. Magn. Reson.* **76,** 149–154 (1988).